Spatio-temporal dynamics of $PM_{2.5}$ and PM_{10} concentrations in a complex urban environment recorded by mobile monitoring for the example of Karlsruhe, South-West Germany

Xiao Wang · Junwei Song · Harald Saathoff · Reiner Gebhardt · Stefan Norra

Abstract The spatial distribution of particulate matter pollution in urban areas is as complex as the complexity layout of buildings and streets and the various emission sources. Because of relatively high costs and inflexibility, the traditional fixed station monitoring is not able to satisfy the demand of dynamic particulate monitoring. A particulate sensor (OPC_N3) was installed on a trailer of a bicycle and applied to investigate spatio-temporal distributions of $PM_{2.5}$ and PM_{10} concentrations in summer time of Karlsruhe, Germany. Before that, the sensors were calibrated against a standard instrument (Fidas200). Temporal variations show that $PM_{2.5}$ and PM_{10} mass concentrations in the morning were on average higher 2.7 ± 1.2 µg/m^3 than in the afternoon and evening. The highest $PM_{2.5}$ and PM_{10} concentrations were observed in the southern forest of Karlsruhe (segment 9), and the street surface is the primary influencing factor. Walking at 5 km/h has a higher concentration than speed at 5 km/h of riding. When riding at different speeds on the same gravel and potholed path, higher speeds are associated with higher particulate matter (PM) concentrations. Distribution pattern of particulate matter on workday and weekend was also different: Mean $PM_{2.5}$ and PM_{10} concentrations of southern forest (segment 10) in the morning and evening at weekend are on average higher by 11.2 ± 10.3 µg/m^3 than at workday. Construction activities on workday also had significant effect on particulate matter concentration. Spatial distribution of aerosol concentrations was highly depending on land use and city structure. These results provide good insights for the application of low-cost sensors

X. Wang (✉) · S. Norra
Division of Soil Science and Geoecology, Institute of Environmental Sciences and Geography, University of Potsdam, 14476 Potsdam, Germany
e-mail: xiao.wang@uni-potsdam.de

S. Norra
e-mail: stefan.norra@uni-potsdam.de

X. Wang · S. Norra
Working Group Environmental Mineralogy and Environmental System Analysis, Institute of Applied Geosciences, Karlsruhe Institute of Technology, 76131 Karlsruhe, Germany
e-mail: stefan.norra@uni-potsdam.de

J. Song · H. Saathoff
Institute of Meteorology and Climate Research, Karlsruhe Institute of Technology, Eggenstein-Leopoldshafen 76344, Germany
e-mail: junwei.song@ircelyon.univ-lyon1.fr

H. Saathoff
e-mail: harald.saathoff@kit.edu

R. Gebhardt
Institute of Geography and Geoecology, Karlsruhe Institute of Technology, Karlsruhe 76131, Germany
e-mail: reiner.gebhardt@kit.edu

in urban environments monitoring and a basis to develop potential mitigation measures.

Keywords Urban environment · Building structure · Mobile monitoring · Particulate matter · PM sensor

Introduction

Particulate matter pollution has negative health effects, causing diseases such as lung cancer and respiratory illness, especially in the urban areas. Páez-Osuna (2022) showed that the COVID-19 mortality rate has a positive association with $PM_{2.5}$ concentration and population density in Sinaloa, Mexico. Ghahremanloo et al. (2022) showed that decreasing in human mobility resulted in reductions in $PM_{2.5}$ levels. The COVID-19 pandemic mobility restrictions resulted in $PM_{2.5}$ reductions of 35%, 29%, and 19% in Wuhan City, Hubei Province (Wuhan excluded), and China (Hubei excluded), respectively (Chu et al., 2021). Research found out that the concentrations of NO_2 in most cities worldwide decreased in varying intensities during COVID-19 lockdown: London decreased by 42% (Dacre et al., 2020), Roma decreased by 27% (Shi et al., 2021), Madrid and Barcelona in Spain by 62% and 50%, respectively. Pattinson et al. (2014) found that for ultra-fine particles (UFP), CO and PM_{10}, arterial roads featuring shops and numerous intersections with traffic lights had a stronger influence on concentrations than the busier but more free-flowing highways.

However, PM concentrations can vary depending on local emissions, land use, building pattern, and atmospheric conditions, resulting in spatial and temporal variability in air quality over relatively small areas (Norra et al., 2023; Wu et al., 2022; Zikova et al., 2017). Thus, low-cost sensors for mobile monitoring have an enormous potential and flexibility to investigate complex structures, especially of cities. Many previous studies already confirmed this (Karagulian et al., 2019; Pattinson et al., 2014). Ultrafine particles (UFP) and black carbon (BC) reach peaks near busy cross-roads and in tunnels, and for UFP and BC, a positive relationship was demonstrated between pollutant concentration and traffic intensity (Peters et al., 2014). Spatio-temporal distribution of PM concentration are also closely linked to wind speeds and directions (Song et al., 2022) which become altered by building patterns and influence the PM concentrations distribution.

Many mobile measurements have been reported in various cities around the world. Pochwała et al. (2020) used unmanned aerial vehicles with a low-cost air pollution sensor to measure the vertical distribution of air pollution in Opole city (Poland). They found that there were relatively low concentrations at ground level, but at heights from 60 m upwards, the concentrations of $PM_{2.5}$ and PM_{10} increased significantly up to about 100 m, before the PM concentration rapidly decreases again. Chauhan et al. (2022) used a low-cost sensor to investigate the particulate matter concentrations in the northern parts of India. The concentration of $PM_{2.5}$ ranged from 20 to 92 µg/m^3 and PM_{10} ranged from 22 to 131 µg/m^3. Local industries, dust, and crop residue burning are the main sources of pollution in this area. The relationship between greenspace and personal exposure to PM during walking trips was also reported in Delhi, India (Mueller et al., 2022).

Also, mobile monitoring with low-cost air pollution sensors have been reported for Germany. A cyclists' exposure study in the city of Münster showed that PM_{10} is influenced by the distance to the motorized traffic. Bicycle routes closer to high traffic showed much higher levels of particle exposure than at low traffic areas (Carreras et al., 2020). Samad and Vogt (2020) investigated and analyzed nitrogen oxides (NO and NO_2), ozone (O_3), particulate matter ($PM_{2.5}$ and PM_{10}), ultrafine particles (UFP) and black carbon (BC) pollutants in the city of Stuttgart by combining passive sampler points and mobile monitoring. Birmili et al. (2013), who investigated the particle mass concentrations by mobile measurement in the city of Leipzig, Germany, found that the motor traffic is the major source of the PM. The emissions of smoking and cooking activities in outdoor seating areas of the restaurants both have obvious effects on the particles with a diameter of 0.25 to 1 µm. Coarse mode particle concentrations (diameter of 2.5 to 10 µm) depend on the ability of surfaces to release particles by resuspension. A model based on street view images and mobile monitoring was developed to investigate and analyze the spatial pattern and driving factors of black carbon in the city of Augsburg, Germany (Liu et al., 2021).

Thus, low-cost optical particle sensors can produce meaningful data with high spatial resolution at

low and high temperatures and when in motion and it can be utilized for outdoor monitoring (Levy et al., 2019). The aims of this work are to (1) describe the temporal and spatial distribution characteristics of PM, discuss the influencing factors of PM concentration distributions in summer time, and (2) discuss the impact of gravel and potholes path on PM concentrations in the forest. This study will provide an insight into microspatial variations in summer time across a typical medium size central European city, the city of Karlsruhe, Germany.

Methods and materials

Study areas

Karlsruhe is located in the southwest of Germany and the river Rhine flows east of Karlsruhe. It is almost completely on the Upper Rhine Plain and has about 300,000 permanent residents. Karlsruhe experiences an oceanic climate often influenced by marine air masses and less often by continental air masses. The climate is therefore moderate and humid. The historical average annual air temperature and precipitation are 10.5 °C and 770 mm (Deutscher Wetterdienst). The total area of the city is 173.46 km^2.

The route map for the bike dragged aerosol measurements is shown in Fig. 1. A fixed station was placed at the Durlacher Tor, which is also the start and end point of the bike route. Durlacher Tor is a former city gate, and now, it is the intersection connecting three districts, the Innenstadt-Ost, Oststadt, and Südstadt of Karlsruhe. It is an important crossection for car traffic and trams for people to enter the city center and to leave the city. The tour includes parts of the university, an avenue, park, residential areas, and an urban forest. Therefore, it reflects well the variability of the urban aerosol distributions. The route was sampled at 10 days between 10 and 24 July, 2022, and is about 15 km long. The average of bicycling speed was 6–8 km/h. Dates, times (local), and average meteorological conditions of every bike tour are listed in Table S1.

In oder to explain the results that the route was divided into 20 different sections according to variable classifications based on the land use and the traffic sitation. Further details of the segments are listed in Table 1.

Methodology

Mobile measurement platform

Bike measurements of particulate matter (PM) were carried out with a custom-built sensor box, on the trailer. In this box, a low-cost PM sensor (OPC_N3, Alphasense) was installed for measuring $PM_{2.5}$ and PM_{10} mass concentrations. The OPC_N3 sensor were set to sample at a resolution of 5 s. The total flow rate of the OPC_N3 is 5.5 L/min. The sensor measures scattered light which varies with particle size. Hence, it allows particle counting 24 user-configurable sizing categories in the range of 0.35–40 µm and give the particle size distributions. For further information on the performance of this sensor is provided on the website (Technical Specifications OPC-N3 Particle Monitor, https://www.alphasense.com/products/view-by-target-gas/particulates-optical-particle-counters). The PM sensor was installed inside the box, and there is a rubber tube about 3 cm long at the sampling inlet that passes through the plastic siding of the box and connects to the outside. The PM sensor was positioned at a height of approximately 60 cm above the ground, representing typical conditions that children are exposed to while seated in trailers or riding children's bicycles. A laptop in the box was used to record and save PMs data. It is hot and scorching in July of Karlsruhe, and the sunlight would quickly heat up the inside of the box. To ensure the laptop continued to work properly, we pasted tin foil on the outside of the box and installed a small fan on the side of the box to cool the inside of the box. As well as sensors (Rotronic HygroClip 2 Typ HC2-S3) measured temperature and humidity data. A GPS (BT-Q1000XT, Qstarz GmbH) recorded the location data. Mobile monitoring bike with sensor systems is shown in Fig. S1.

Performance of the OPC_N3 sensor

In order to evaluate the performance of the OPC_N3 sensor, we simultaneously carried out two comparison measurements with an optical particle counter (Fidas200, Palas GmbH) at Durlacher Tor for 10 days. Furthermore, we also collected $PM_{2.5}$ and PM_{10} on filters (the filters were collected during the day and night, respectively, each time lasting approximately 11.5 h) by a Low Volume Sampler

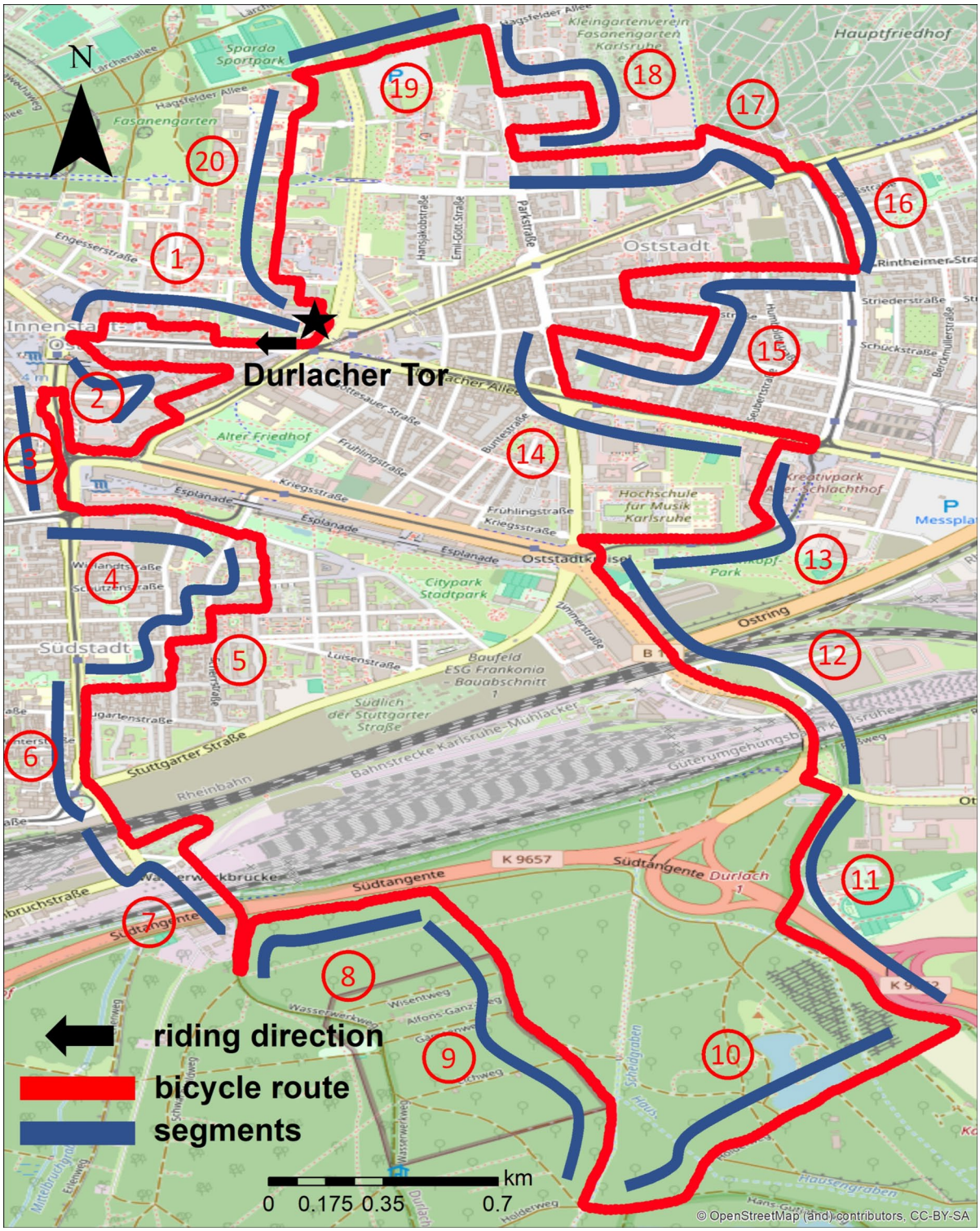

Fig. 1 Map of Karlsruhe with the route of the bike tour and the description of the segments

Table 1 Description of the segments on the measurement route

Segment	Description
1	Durlacher Tor Station (bus station, tram station and subway station), Kaiserstraße (street) and KIT-Campus South (Construction area)
2	Residential area with low traffic and several restaurants and bars located in this area
3	Main street of the south city
4	Area with park and low traffic street
5	Residential area with low traffic
6	Main street of the south city
7	Karlsruhe rail freight terminal area and a bridge linking south city and the forest
8	Path parallel to and adjacent to a highway
9	Gravel and hotholed path covered with scattered and broken leaves in the forest
10	Asphalted path in the forest without traific
11	Asphalted path in the forest (occasionally there are vehicles driving)
12	Karlsruhe rail freight terminal area and the main road connecting expressway (E35 and B3)
13	Park (Otto-Dullenkopf Park) and its surrounding areas
14	Main road (Durlacher Allee and Georg-Friedrich-Straße)
15	Residential area with low traffic
16	Street with moderate traffic
17	Parking lot in greenland and residential area with low traffic
18	Residential area with low traffic
19	Green land and asphalted path without triffic
20	KIT-Campus South

The path in the forest is just for walking and bicycle (area 8, 9, 10), but sometimes also can see municipal transport vehicles driving on the path (During the sampling period, I met with the municipal transport vehicles of the wildlife park once in the morning in area 9)

(LVS, Comde-Derenda GmbH), weighted, and calculated the content. The OPC_N3 sensor was fixed inside the box and put on the roof of measurement container. The sampling inlets of OPC_N3 sensor and Fidas200 were same and located at 2.5 m above the ground. The sampling inlets of Low Volume Sampler were located 3.7 m above ground level and 1.2 m above the container roof. The comparison of $PM_{2.5}$ and PM_{10}, mass concentrations measured by the Fidas200, and the low cost optical particle counter (OPC_N3, Alphasense) shows a very good correlation $R = 0.91$ (RSME = 3.62 μg/m^3), for $PM_{2.5}$ and $R = 0.92$ (RSME = 6.85 μg/m^3) for PM_{10} (Fig. S2), suggesting that the OPC_N3 is reliable for air quality monitoring. However, the slopes are not 1; the OPC_N3 always records higher concentrations. Filter-PM_{10} concentrations show good correlations with OPC_N3-PM_{10} ($R = 0.94$, RSME = 3.34 μg/m^3) and Fidas-PM_{10} ($R = 0.98$, RSME = 0.93 μg/m^3) concentrations during the calibration period. OPC_N3 PM data were higher than the filter-based values while the Fidas200 PM data were always lower compared to the gravimetric data. However, the overall tendency is consistent with the OPC_N3-$PM_{2.5}$ and Fidas-$PM_{2.5}$ concentrations (Fig. S3). Dust events and meteorological factors may affect the accuracy of low-cost sensors (Aix et al., 2023; Kang & Choi, 2024). However, we conducted sampling on dry days with relative humidity below 60%, except for the morning of July 21 (Table S1). In addition, based on the scatter plot comparison between OPC_N3, Fidas 200, and LVS filters measurements, we consider that the low-cost sensor we used is capable of providing a reasonable data quality.

Time series of air temperature and relative humidity, $PM_{2.5}$, and PM_{10} are shown in Fig. 4 to compare the different aerosol measurement types ($PM_{2.5}$ and PM_{10} mass concentrations measured by the Fidas200, OPC_N3, and LVS; temperature and relative humidity data from the DWD (Deutscher Wetterdienst), which were collected from Rheinstetten meteorological station with the code 4177;

wind speed and wind direction data from LUBW (Landesanstalt für Umwelt Baden-Württemberg), which were collected from Karlsruhe-Nordwest meteorological station with the code 4444). Generally, the trends of concentrations of all three measurement types are similar although the concentrations show significant differences. The reason of higher concentrations of the LVS-Filter measurements can be explained by the different techniques. OPC_N3 and Fidas200 are optical sensors cutting strictly at 2.5 µm and 10 µm, respectively, whereas the LVS sampling has a S-shaped cut off curve with a transmission of 50% at these specific thresholds. This means that active sampling on a filter does not exclude all larger particles to be collected, although the contribution of these larger particles decreases by increasing size. In addition to that, also relative humidity influences the samples differently. Hygroscopic particles will absorb water. In the case of the LVS sampling, the filters are exposed to the ambient relative humidity as long as they are operating in the sampling system. In case of Fidas200 and OPC_N3, the particles are analyzed in situ and on-line. Figure S4 shows the variations of relative humidity over the time of the campaign. Nevertheless, the comparison of the different PM measurement techniques shows that they result in similar trends over time. Since the aim of this study is not to study the legal limits of $PM_{2.5}$ and PM_{10} but the spatial trends of PM loads in the atmosphere due to traffic and land-use in a city region, the OPC certainly can be used for this task. Regarding the general time series in June 2022, $PM_{2.5}$ and PM_{10} mass concentrations experienced a rapid growth reaching peaks at around 1 am of 19th June, then remaining at high concentration levels until 20th June. A 24-h backward trajectory (Fig. S5) illustrates that air mass reaching Karlsruhe were mainly from southeast direction.

Data processing

The data of moving average PMs concentrations at 5 s resolution are available from the OPC_N3 sensor. The data with a resolution at 30 m were processed by MATLAB 2022b (MathWorks) used for the final analysis. ArcGIS 10.8 (ESRI) and Origin 2021 (OriginLab) software were used to plot the figures.

Quality control and quality assurance

The 10-day comparison measurements between the OPC_N3 sensor and the Fidas200 and Low Volume Sampler were used to evaluate the performance of the OPC_N3 sensor. Before commencing each measurement campaign, we conduct a thorough inspection of the mobile measurement systems to ensure that the instruments' connections remain uninterrupted during each campaign, thereby maintaining the continuity of data recording. Random impact factors (e.g., construction, resuspended dust caused by wheels on gravel and potholed path) were recorded during the campaigns, affected data caused by random factors was also kept and analyzed in this study. Random factors contribute to the complexity of the environment and can also provide insight into its actual condition.

Segment 9 is gravel and potholed path covered with scattered and broken leaves in the forest. Since our sensor was installed at a relatively low height (60 cm) above the ground, it can simulate exposure conditions for children riding bicycles or laying in a trailer. However, when moving on unpaved and uneven path, the measurements may be influenced by resuspended particles generated by the wheels. In order to better explore the impact of resuspended dust on particulate matter concentration. This segment was divided into 3 different parts (parts A, B, and C) depend on the path condition (Fig. 7). They are long ~ 280 m, ~ 140 m, and ~ 400 m for parts A, B and C, respectively. The road surface in part A has been damaged and is covered with gravel mixed with broken leaves and a small amount of soil. Part of the road surface in part B has been damaged and is covered with gravel mixed with broken leaves; there also have some potholes. The sitution of part C is better than parts A and B, coverd with some potholes. There are some potholes on the road, but not too much gravel. Considering the impact of resuspended dust on sensors, we designed different riding/wheeling speeds (wheeling at the spped of 5 ± 0.5 km/h, riding at the speed of 5 ± 0.5, 7 ± 0.5, and 9 ± 0.5 km/h, respectively) to evaluate the effect of speed on particulate matters concentrations. Speed recorder was used to monitor and keep the riding/sheeling speed. We did the samplings of this part from 9:00 to 11:20 am on 19th July 2022. The different riding speeds were measured in the same section and same direction.

Results

Median PM concentrations

The minimum, maximum, first quartile, third quartile, average, and median values of $PM_{2.5}$ and PM_{10} mass concentrations records of every bike tour are shown in Fig. 2. The highest $PM_{2.5}$ concentrations were measured on the morning (7:42–9:57 am) of 21st July with 20.7 μg/m^3. We recorded that road construction was underway less than 2 m from our mobile trailer. The highest PM_{10} concentration was occurred on the morning of 17th July with 134 μg/m^3. We encountered a municipal vehicle on a narrow road (segment 9). The driver drove the car on the dirt side of the road to avoid us. Resuspended dust has a great impact on the PM10 concentration caused by the car wheels. Mean $PM_{2.5}$ concentrations of those bike tours (10–24 July) vary from 1.0 to 5.7 μg/m^3. Mean PM_{10} concentrations of those bike tours vary from 6.8 to 25.3 μg/m^3. The largest range for $PM_{2.5}$ was observed on the morning of 21st July and for PM_{10} on the morning of 17th July. Furthermore, the $PM_{2.5}$ and PM_{10} have relatively higher mean concentrations in the morning than others times of the day.

The median is less affected by extreme values by strong local pollution sources, such as construction activity and high-emitting vehicles (Choi et al., 2013; Pattinson et al., 2014). The spatial distribution of median $PM_{2.5}$ and PM_{10} concentrations for 17 bike tours is shown in Fig. 3. A significant spatial variation of the PM concentrations can be seen from the results. $PM_{2.5}$ and PM_{10} concentrations have the similar spatial distributions. The peak values of 4.37 and 46.2 μg/m^3 for $PM_{2.5}$ and PM_{10} respectively were observed in segment 9. The lowest $PM_{2.5}$ concentrations (1.5–2.0 μg/m^3) were measured in the residential area (segment 18) and the KIT-Campus South (segment 20). Relatively high PM_{10} concentrations (10–20 μg/m^3) were measured at KIT-Campus South (segment 1), in the residential area (segment 2), a freight terminal area (segment 7), and Otto-Dullenkopf Park (segment 13).

Spatio-temporal distribution of particulate matter mass concentrations

As illustrated in Fig. 4a, there are several areas with high $PM_{2.5}$ concentrations (> 3.5 μg/m^3) especially in the morning, the highest concentrations in the southern forest, especially on the gravel path, which was covered with scattered and broken leaves. This location will be discussed in section of speed effect on potholed path. The highest $PM_{2.5}$ concentrations (6.93 μg/m^3) also appeared around the stationary monitoring site at Durlacher Tor, because there were continuous road repairs and building constructions. Karlsruhe is hot and blazing at noon and in the afternoon in July, and the outdoor construction activities are usually carried out in the morning (we record this situation during the sampling period). During the morning, the temperature was about 20 ℃ and no

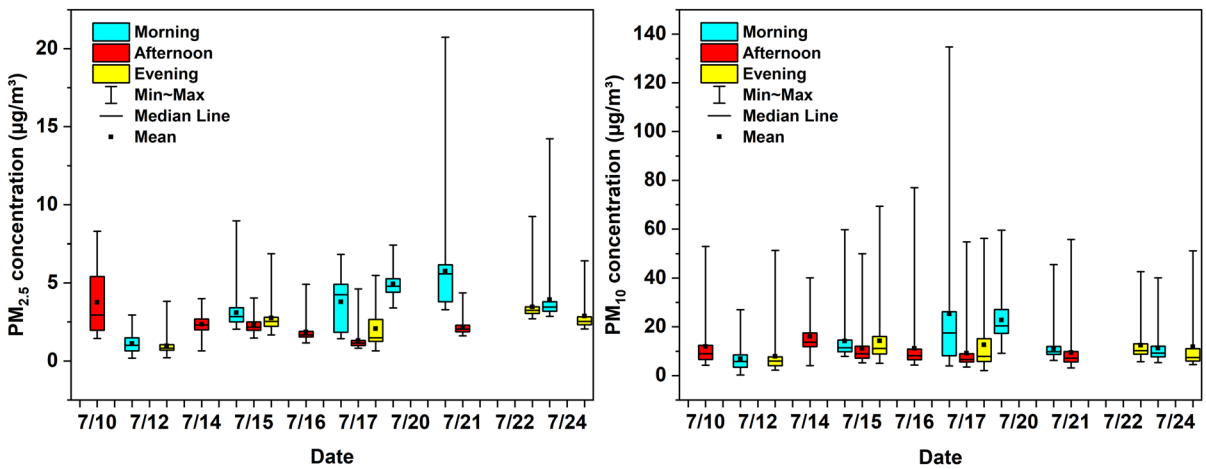

Fig. 2 $PM_{2.5}$ and PM_{10} mass concentrations statistics of all bike tours

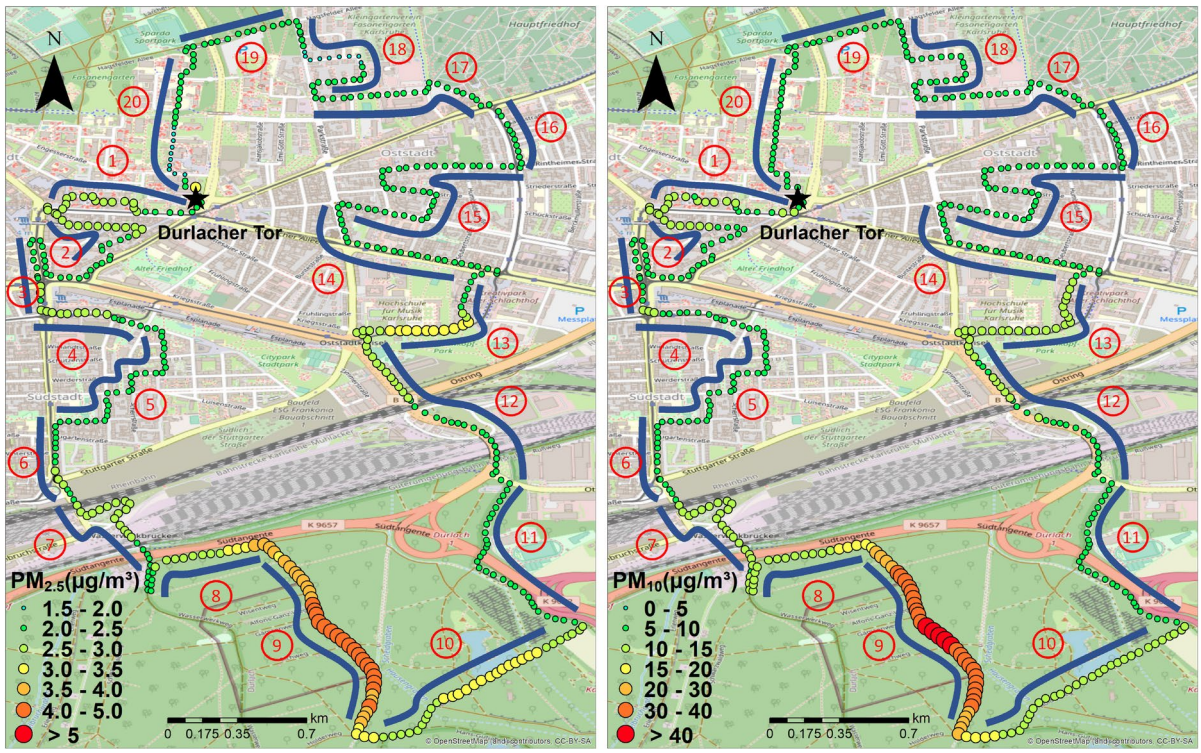

Fig. 3 Median $PM_{2.5}$ and PM_{10} concentrations (µg/m^3) of 17 bike tours in Karlsruhe

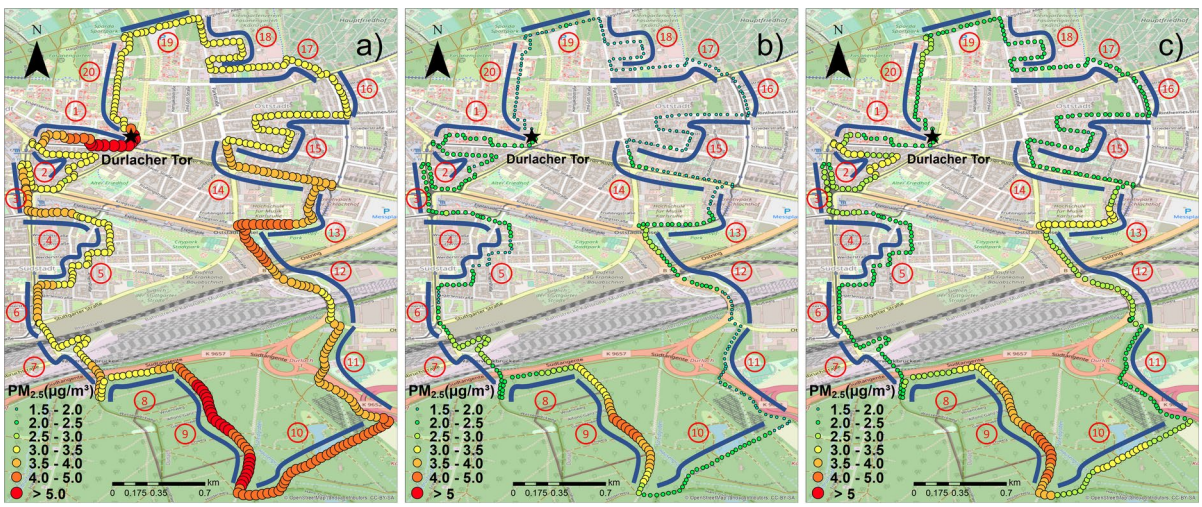

Fig. 4 Median $PM_{2.5}$ concentrations (µg/m^3) of 17 bike tours in Karlsruhe—**a** morning, **b** afternoon, and **c** evening

strong sunlight. This is the peak period of construction that releases a large number of fine particulates into the atmosphere. Around the Otto-Dullenkopf Park (Segments 12 and 13), $PM_{2.5}$ concentrations were relatively high (>4 µg/m^3) and there is a busy intersection. Three main roads, Wolfartsweierer Str., Ludwig-Erhard-Allee, and Stuttgarter Str., are connected here. Wolfartsweierer Str. is the entrance and

exit of the expressway and one of the most frequented roads leading through Karlsruhe that traffic volumes are ~ 31,000 for 24 h (Stadt Karlsruhe, 2013).

Figure 4b shows the results for the afternoon, the highest $PM_{2.5}$ concentrations was measured on the gravel path of the forest (segment 9), ranging from 4.0 to 5.0 μg/m^3. Relatively high $PM_{2.5}$ concentrations recorded in rail freight terminal area (segment 7), ranging from 2.5 to 3.0 μg/m^3. Within the residential area (segments 5, 15, and 18) and the KIT-Campus South (segment 20), show the lowest $PM_{2.5}$ mass concentrations. During the evenings, the spatial distribution of $PM_{2.5}$ is very similar to that in the mornings.

The spatio-temporal distributions of median PM_{10} concentrations are shown in Fig. 5. PM_{10} has similar distributions as $PM_{2.5}$. PM_{10} has a high concentration (> 30 μg/m^3) in the animal park (segment 9) all the day. It is found that the Otto-Dullenkopf Park (segment 13) has relatively high concentrations (20–30 μg/m^3) during the evening, because there is a big gravel parking lot and a lot of people had a walk and did some activities in the park. A 3-day African Summer Festival was held during the sampling period (15–17 July) and attracted many participants. This was high-traffic areas in the evening compared to the morning and afternoon. We recorded, the PM_{10} concentration distributions during the evening were higher than in the morning and in the afternoon.

$PM_{2.5}$ and PM_{10} concentration distributions also show the variety in different mornings (Figs. S6 and S7). On the morning of 12th July, low $PM_{2.5}$ concentrations (≤ 2.5 μg/m^3) were recorded during the 17 times bike tours, and the low PM_{10} concentrations (≤ 8 μg/m^3) were recorded at most segments of this campaign except for the segments 1, 2, 7, and 9. On the morning of 15th July, the highest $PM_{2.5}$ (8.7 μg/m^3) and PM_{10} (59.4 μg/m^3) concentrations were recorded close to the Durlacher Tor Station. Besides, the highest PM_{10} concentrations (134.1 μg/m^3) were observed in segment 9. $PM_{2.5}$ and PM_{10} concentration distributions were similar on the morning of 17th July; low concentrations ($PM_{2.5} \leq 2.5$, $PM_{10} \leq 8$ μg/m^3) were recorded in the west (segments 1–6), and high concentrations ($PM_{2.5} > 3.5$, $PM_{10} > 16$ μg/m^3) were seen, especially in the southern forest (segments 9 and 10) and east city (segments 13 and 14). Relatively higher $PM_{2.5}$ and PM_{10} concentrations were observed along the whole bike tour on the morning of 20th July. On the morning of 21st and 24th July, the $PM_{2.5}$ concentrations recorded in south-west areas that were higher than in north-east areas. The highest concentrations of PM_{10} (41.5 μg/m^3) were on KIT campus (segment 1) on the morning of 21st July and high concentrations of PM_{10} (> 12 μg/m^3) occurred in the southern forest (segments 9 and 10).

$PM_{2.5}$ and PM_{10} concentration distributions in the afternoons are shown in Figs. S8 and S9. $PM_{2.5}$ and PM_{10} concentrations in south-west areas were higher than in north-east areas on the afternoon of 10th July. $PM_{2.5}$ and PM_{10} concentrations show the

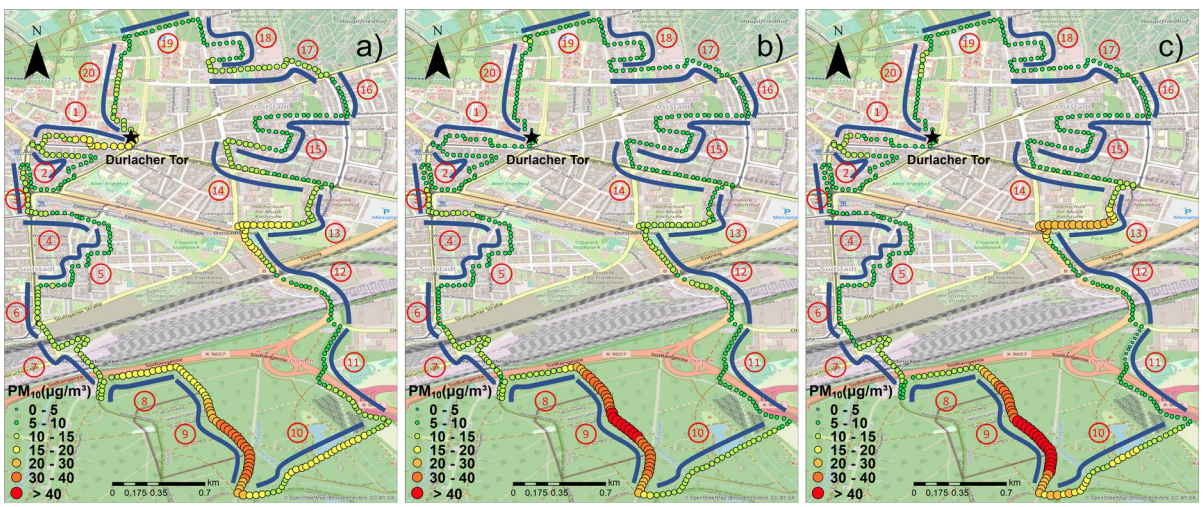

Fig. 5 Median PM_{10} concentrations (μg/m^3) of 17 bike tours in Karlsruhe—**a** morning, **b** afternoon, and **c** evening

similar patterns on 14th July; the relatively high $PM_{2.5}$ (> 3.5 μg/m^3) and PM_{10} (> 24 μg/m^3) concentrations were measured in the southern forest (segments 9 and 10) and the residential areas in the eastern city (segment 15). Furthermore, $PM_{2.5}$ concentrations have the similar distribution patterns in the afternoon of 15th and 16th July. For PM_{10} concentration distribution on the afternoon of 15th July, the extremely high PM_{10} concentrations (> 24 μg/m^3) occurred in the southern forest (segments 9 and 10) and the relatively low PM_{10} concentrations (8–12 μg/m^3) distributed in segments 2–5. Relatively high PM_{10} concentrations (12–20 μg/m^3) were observed in the intersection between segment 12 and segment 13 of 16th July. $PM_{2.5}$ concentration distribution patterns were similar on 17th and 21st July, but $PM_{2.5}$ concentrations on 17th July were lower than on 21st July. Relatively low PM_{10} concentrations (4–8 μg/m^3) were observed on the bridge in segment 7 and 12.

$PM_{2.5}$ and PM_{10} concentration distributions in the evenings are shown in Figs. S10 and S11, respectively. Low $PM_{2.5}$ concentrations (≤ 2.5 μg/m^3) were measured in the whole bike tour on the evening of 12th July. We recorded low PM_{10} concentration (≤ 8 μg/m^3) in the whole route except segments 9 and 13 on the evening of 12th July. Low $PM_{2.5}$ concentration (≤ 2.5 μg/m^3) was observed in the residential aeras (segments 5, 15, and 18) on the evening of 15th and 17th July. High PM_{10} concentration (> 16 μg/m^3) occurred in KIT campus (segment 1), southern forest (segment 9 and 10), and Otto-Dullenkopf Park (segment 13) on the evening of 15th and 17th July. The range value from 1.5 to 3.5 μg/m^3 of $PM_{2.5}$ concentration was observed during the whole measurement campaign on 22nd July. The highest PM_{10} concentrations were measured on the path along the highway (segment 8) and southern forest (segment 9) on the evening of 22nd July. The highest $PM_{2.5}$ concentration (6.4 μg/m^3) was measured in Otto-Dullenkopf Park (segment 13), and relatively high concentration (3.5–4.5 μg/m^3) were observed in the residential area (segment 2) and southern forest (segments 9 and 10) of 24th July. The extremely high PM_{10} concentrations (> 24 μg/m^3) were measured in the southern forest (segments 9 and 10) and Otto-Dullenkopf Park (segment 13) on the evening of 24th July.

Figure 6 shows the statistical values of $PM_{2.5}$ and PM_{10} concentrations for different segments in the morning, afternoon, and evening during the period of bike tours. It is observed that concentration range of $PM_{2.5}$ at segment 1 is the largest, varying from 0.2 to 20.7 μg/m^3, and mean value (5.9 μg/m^3) is also the highest of all. Construction activities lasted during bike tours period, especially in the morning.

Within green areas (segments 8, 9, 10, 11, 17, and 19), segment 9 has the highest average values of PM_{10} in the morning (42.0 μg/m^3), afternoon (34.5 μg/m^3) and evening (35.9 μg/m^3) and $PM_{2.5}$ in the afternoon (4.0 μg/m^3) and evening (3.6 μg/m^3). Segment 10 has relatively high average PM_{10} concentration values in the morning (18.4 μg/m^3), afternoon (14.1 μg/m^3), and evening (17.3 μg/m^3). The coverage of underlying surface has a great influence on PM concentrations, since segment 9 was a gravel path and covered with scattered and broken leaves. When the bicycle passes through gravel path in this area, the dust that was resuspended by the wheels has a great impact on the concentrations of $PM_{2.5}$ and PM_{10}. Meanwhile, branches of trees on both sides of the path in segments 9 and 10 have extended to the middle of the path, and the dispersal of particulate matter on the leaves and part of the pollen has a certain impact on concentration of $PM_{2.5}$ and PM_{10}. Green areas along segments 11, 17, and 19 have relatively low PM concentrations all the time.

It can be seen in Fig. 6a, c, e that the $PM_{2.5}$ concentrations at all segments in the morning are higher (0.4–3.8 μg/m^3) than in the afternoon and in the evening. Different residential areas also show different distribution patterns. The average $PM_{2.5}$ and PM_{10} concentrations of residential area with several restaurants and bars (segment 2) were 0.6–0.9 μg/m^3 and 3.1–3.4 μg/m^3 respectively higher than other residential areas without restaurants (segments 5, 15, and 18) in the evening, suggesting that outdoor seating areas of a restaurant in the community have some impact on the concentrations of $PM_{2.5}$. We found that segment 13 had a higher average $PM_{2.5}$ and PM_{10} concentration in the evening ($PM_{2.5}$ = 3.1, PM_{10} = 19.7 μg/m^3) than in the afternoon ($PM_{2.5}$ = 2.1, PM_{10} = 11.0 μg/m^3). Here is a large park (Otto-Dullenkopf Park) with a gravel parking lot. The Africa Summer Festival lasted three evenings (15–17 July) in the Otto-Dullenkopf Park during the campaigns, and attracted many people to participate. The surface of the parking lot was covered with gravel and dirt, and as cars moved slowly, the resuspended dust caused by wheels likely influenced the concentrations of $PM_{2.5}$ and PM_{10}.

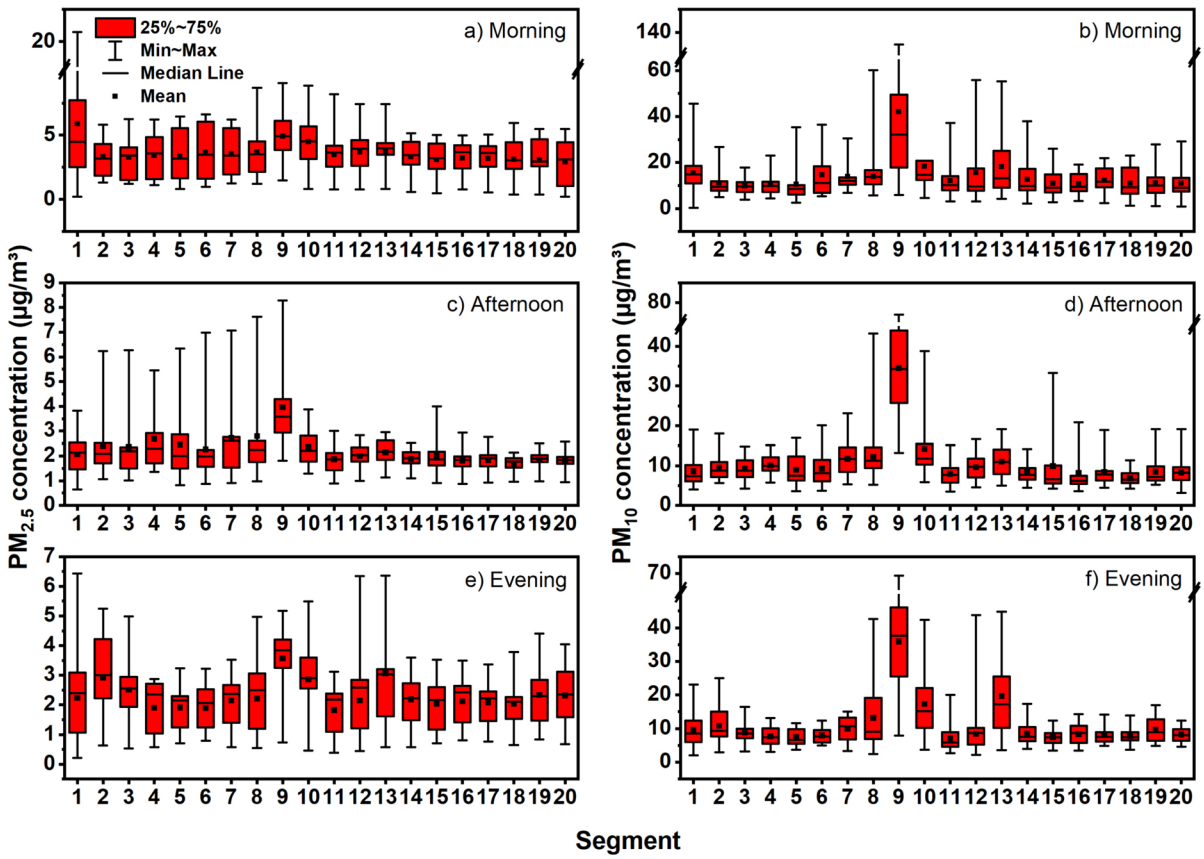

Fig. 6 Statistical parameters of $PM_{2.5}$ (left) and PM_{10} (right) mass concentrations in different segments during morning, afternoon, and evening hours for the whole measurement campaign (17 routes)

Speed effect on potholed path

Table 2 shows the mean ± standard deviation and minimum and maximum $PM_{2.5}$ and PM_{10} mass concentrations measured for different bike tours in segment 9. For wheeling the bike, mean $PM_{2.5}$ and PM_{10} mass concentrations are 6.38 ± 1.49 and 76.89 ± 34.39 μg/m^3, respectively. For riding, it is easy to see that faster speed biking recorded higher PM_{10} concentrations. Speed at 5 km/h of riding had the lowest $PM_{2.5}$ and PM_{10} mean values are 4.19 ± 1.66 and 37.82 ± 23.69 μg/m^3, separately. Speed at 9 km/h of riding recorded the highest $PM_{2.5}$ and PM_{10} mean values are 5.43 ± 1.31 and 68.58 ± 28.09 μg/m^3, separately. Measurement at 5 km/h of wheeling the bike recorded mean and max $PM_{2.5}$ and PM_{10} concentrations is also higher than the mean and max value at 9 km/h of riding.

Visualization of $PM_{2.5}$ and PM_{10} mass concentrations records of segment 9 with different speed is

Table 2 Concentrations of $PM_{2.5}$ and PM_{10} (μg/m^3) records of different speed bike tours from 9:00 to 11:20 am on 19th July 2022

	$PM_{2.5}$			**PM_{10}**		
	Mean ± SD	Min	Max	Mean ± SD	Min	Max
5 ± 0.5 km/h wheeling	6.38 ± 1.49	3.22	8.64	76.89 ± 34.39	25.47	140.8
5 ± 0.5 km/h riding	4.19 ± 1.66	2.38	7.08	37.82 ± 23.69	16.49	83.56
7 ± 0.5 km/h riding	5.35 ± 1.48	3.0	7.51	52.03 ± 24.9	18.39	90.19
9 ± 0.5 km/h riding	5.43 ± 1.31	2.73	7.28	68.58 ± 28.09	14.01	115.0

shown in Fig. 7. $PM_{2.5}$ and PM_{10} concentration measurements show the divergences at different speeds. At 5 km/h of wheeling, two high $PM_{2.5}$ mass concentration areas recorded in areas A and B, PM_{10} reached the highest concentration (140.8 μg/m^3) in area B and recorded serval medium value concentration (68–86 μg/m^3) in other areas. For the 5 km/h riding tour, $PM_{2.5}$ had a relative higher concentration (6–8 μg/m^3) in areas A and B, and a low concentration (2–4 μg/m^3) in other areas. PM_{10} concentration at 5 km/h riding tour had a medium concentration (68–86 μg/m^3) in areas A and B and a relative lower concentration (14–32 μg/m^3) in area C. For 7 km/h riding tour, $PM_{2.5}$ recorded a high concentration (7–8 μg/m^3) in areas A and B, then had a decreasing trend from area B to end. But PM_{10} concentration increased from the north to south, reached the peak value (90.19 μg/m^3) at area C, then decreasing. At 9 km/h of riding, spatial distribution of $PM_{2.5}$ and PM_{10} increased from north to south, reached the peak value at area C, then presented a decreasing trend. In general, spatial distribution of $PM_{2.5}$ and PM_{10} measured at 5 km/h of riding had the similar spatial distribution tendency with 7 km/h of riding but was less in average values ($PM_{2.5}$ = 5.35 μg/m^3 and PM_{10} = 52.03 μg/m^3). $PM_{2.5}$ and PM_{10} distribution

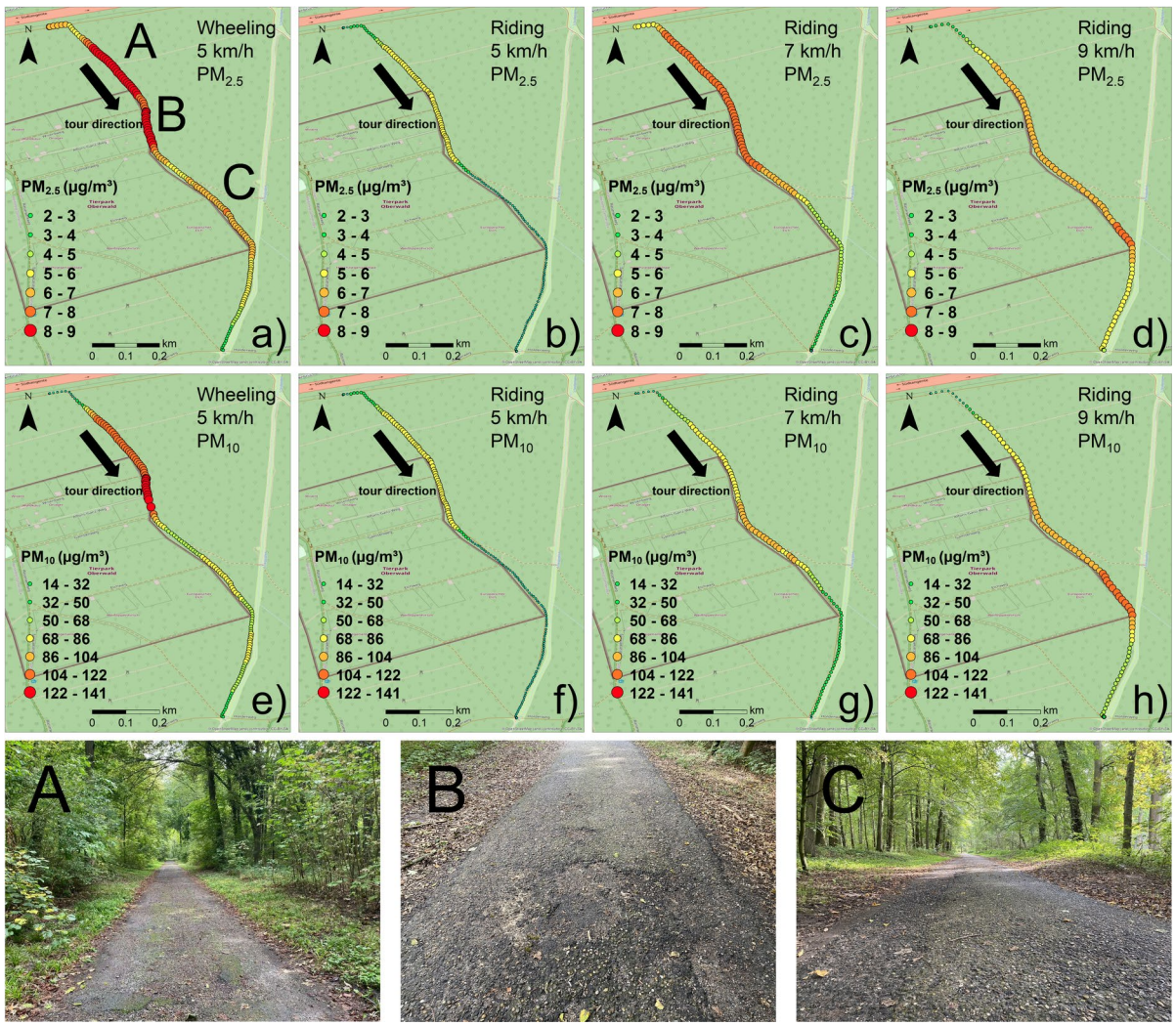

Fig. 7 Spatial resolution with different speed variation and path situation in segment 9 (the different speed of biking or wheeling were recorded from 9:00 to 11:20 am on 19th July 2022)

measurements at 9 km/h had relatively high concentration throughout the segment 9.

Pearson correlation coefficients is used to measure the strength of the association between the variables (Dubey et al., 2022). The results are presented in Fig. 8 ($N=690$, p-values ≤ 0.05). A weak positive correlation occurs between speed and $PM_{2.5}$ and PM_{10} concentrations in segment 9. Correlation value between speed and PM_{10} ($R=0.22$) is similar with the correlation value between speed and $PM_{2.5}$ ($R=0.21$).

Path condition and $PM_{2.5}$ and PM_{10} concentrations at segment 9 are shown in Fig. 7A–C. Some parts of this path have fallen into disrepair over the years, although made of stone and cement. Gravel, soil, potholes, and broken leaves scattered on the path in area A. The path condition in area B is better than area A, but some road uneven and covered with leaves Fig. 7B. The sensor was assembled rear of the bicycle, when the cyclist walked the bicycle pass the potholed path. The front wheel and the cyclist's feet floats ground dust into air firstly. Then rear wheels also float dust from ground. In addition to wheel-induced resuspension particulate matter from potholed path, the personal activity cloud can also contribute to the resuspension of particulate matter. Rodes et al. (1991) reported that the "personal activity cloud" effect can lead to measured concentrations being 1.2–3.3 times higher than ambient levels in residential settings.

The sensor not only measures the content of PM in air but also measures the content of dust resuspended from the ground. That explains why measurements at 5 km/h of walking have a higher concentration than speed at 5 km/h of riding. When riding at different speeds on the same path, higher speed with more dust behind the tires resuspends into air from gravel and bumpy path; measurements at 5 km/h and 7 m/h prove this.

Discussion

High-resolution mobile monitoring data of $PM_{2.5}$ and PM_{10} are obtained by low-cost sensor OPC_N3 in urban areas of Karlsruhe. Three main affirmations can be made: (1) $PM_{2.5}$ and PM_{10} patterns were generally similar, but divergences within special areas also occur, (2) $PM_{2.5}$ and PM_{10} patterns present temporal distribution difference even within 1 day, (3) $PM_{2.5}$ and PM_{10} patterns are influenced by multiple factors, such as weather condition, underlying surface condition and human activities. $PM_{2.5}$ and PM_{10} have the high dynamics of aerosol sources in urban environment, which is the result of the interaction between building structures and human activities and meteorological conditions (Norra et al., 2023).

It is necessary to mention that although the $PM_{2.5}$ and PM_{10} concentrations are generally lower

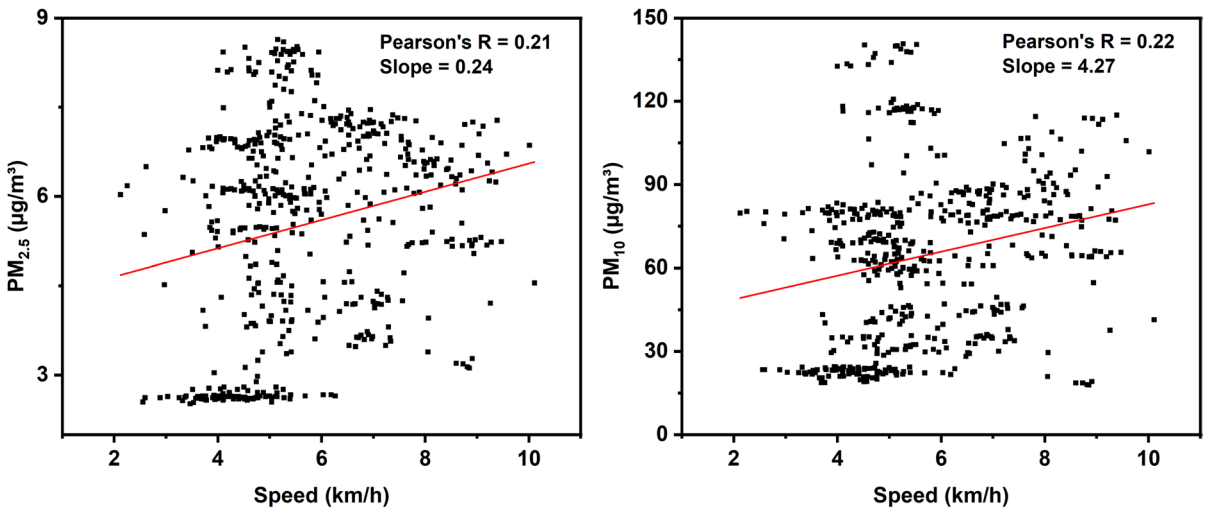

Fig. 8 Scatter plots of $PM_{2.5}$ and PM_{10} mass concentrations and speed and the correlation coefficients of those data in segment 9 from 9:00 to 11:20 am on 19th July 2022

($PM_{2.5} \leq 2$, $PM_{10} \leq 8$ μg/m^3) in residential areas, there are also exceptions. Even in case of low traffic in the residential areas, also green areas, building height and density, parking lot location, distance from the main road, and construction activities also are potential influencing factors. Within residential areas (segments 2, 5, 15, and 18), along segment 2 occurred relative higher $PM_{2.5}$ concentrations (> 3.5 μg/m^3) in the afternoon and evening than at the other three sections. We found that the residential area is located close to the main road and has narrow distance between two buildings; besides, there also has a restaurant open in the noon and evening.

$PM_{2.5}$ and PM_{10} concentrations showed interesting distribution pattern for workday and weekend during this sampling period (Figs. 9 and 10 and Tables S2–S3). Mean $PM_{2.5}$ and PM_{10} concentrations of southern forest (segment 10) in the morning and evening at weekend are higher than at workday. Mean $PM_{2.5}$ and PM_{10} concentrations of segment 1 at workday are higher than Sunday, as we mentioned that road repair and building construction were continued at workdays during the mobile monitoring. At residential area (segment 2), mean $PM_{2.5}$ and PM_{10} concentrations at weekend were higher than workday in the evening. This area located several restaurants and bars and always provide service outside. People enjoy their leisure time during the weekend evening and eating outside with the cool weather, that emission from restaurants would has some effect on the PM concentration. On the main street of south city (segment 3), $PM_{2.5}$ concentrations at workday were higher than weekend in the morning and afternoon, but in the evening, the situation is opposite. Emissions from cars, restaurants, and other sources contribute to a portion of particulate matter during workdays, and at

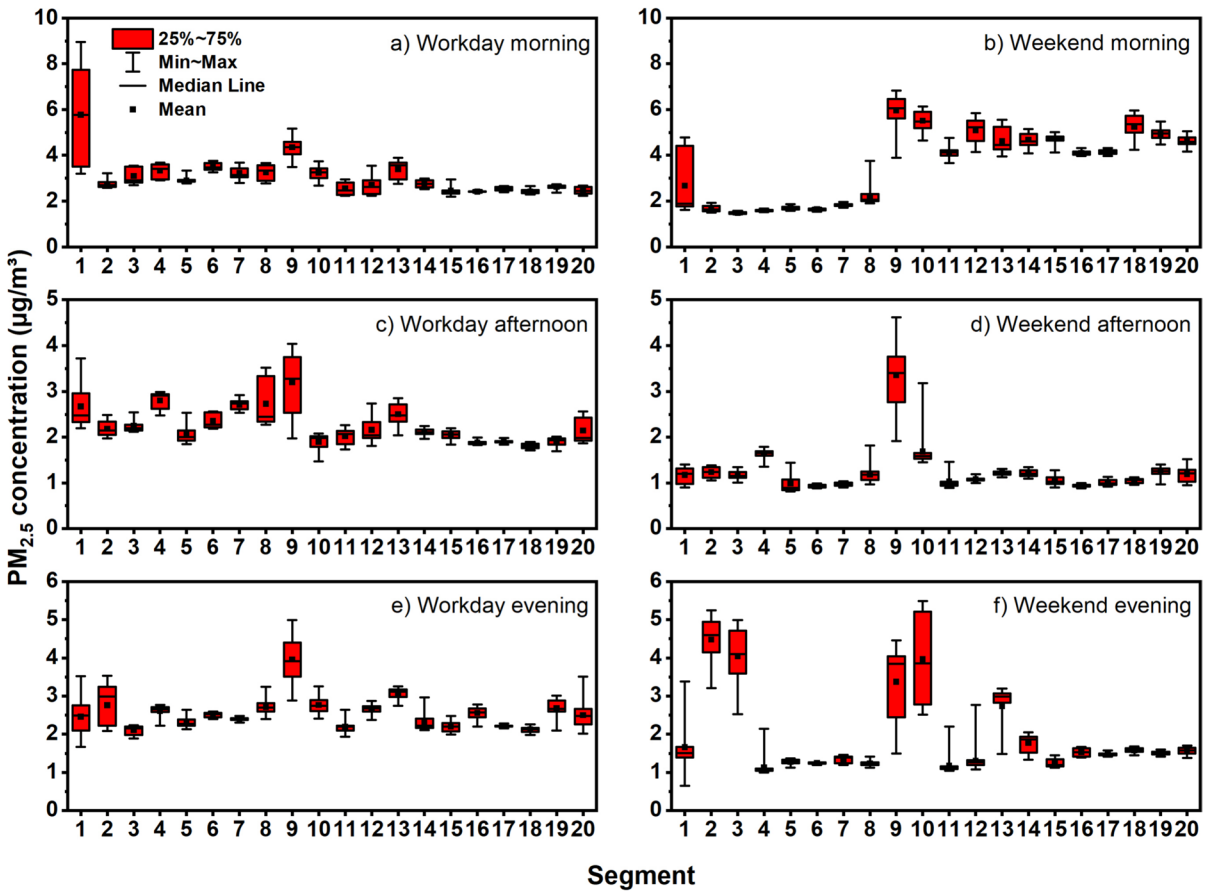

Fig. 9 $PM_{2.5}$concentration in the morning, afternoon, and evening during workday (Friday, 15 July 2022) and weekend (Sunday, 17 July 2022)

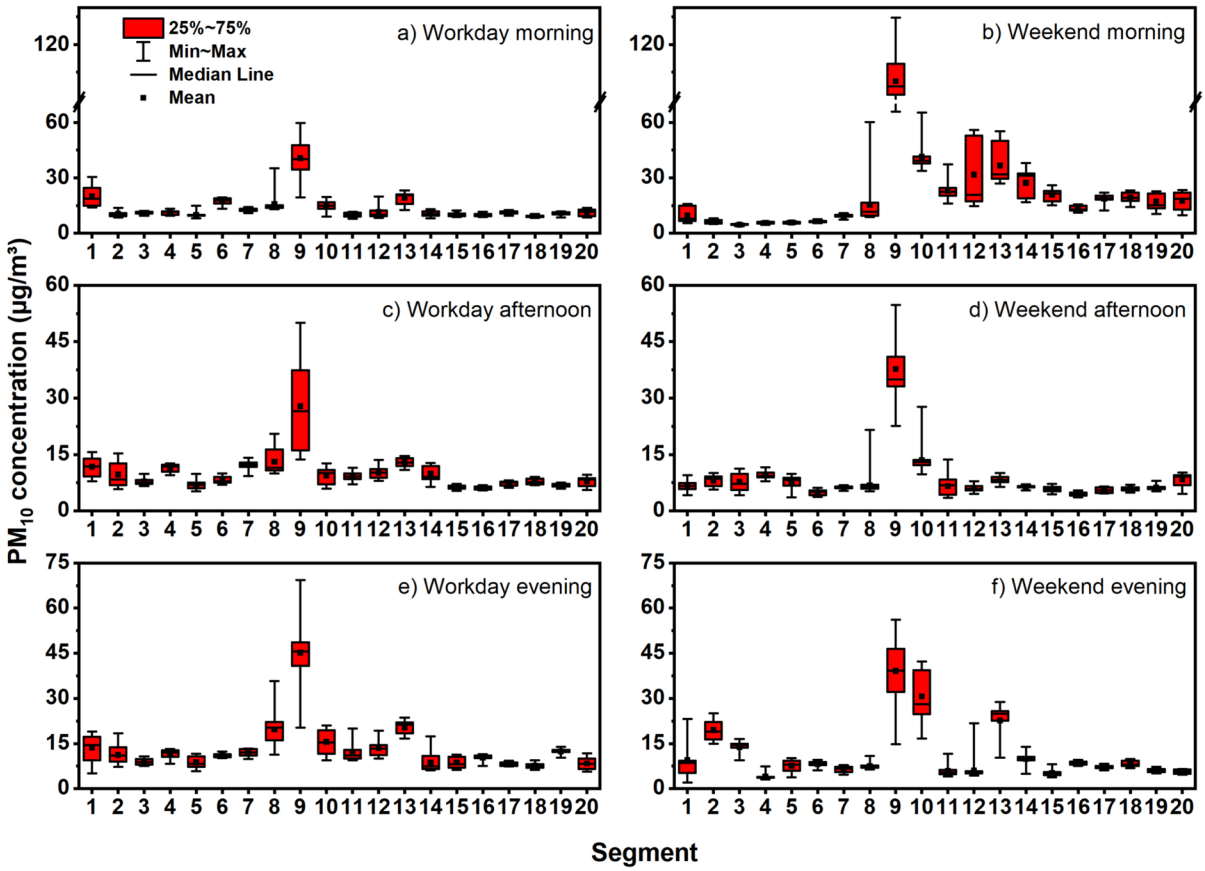

Fig. 10 PM_{10} concentration in different segments in the morning, afternoon, and evening during workday (Friday, 15 July 2022) and weekend (Sunday, 17 July 2022)

weekend, people more like to go outside in the cool evening. The distribution of PM concentration varies among different residential areas, as the concentration of PM was influenced by various factors such as the shape and greenery of the residential area. The $PM_{2.5}$ and PM_{10} concentrations of weekend–weekday comparison only represented as a preliminary observation during the sampling period; more repeated sampling is needed to establish robust differences.

Human activities have an obvious effect on the $PM_{2.5}$ and PM_{10} concentrations. The construction activities constantly occurred during the sampling period. Building and road constructions in segment 1 confirmed this point. Usually, the constructions start in the early morning and end at the noon on the workdays. The highest $PM_{2.5}$ content during construction was above 20 μg/m^3, much higher than that during non-construction periods (the highest content in the afternoon and evening are 3.82 and 6.43 μg/m^3, respectively). PM_{10} concentration reached a peak value (22.6 μg/m^3) in segment 13 in the evening during the Africa Summer Festival, which is about 2 times higher than the concentration (9.08 μg/m^3) before African Summer Festival in the evening. Samad and Vogt (2020) found that the PM_{10} concentration was above 75 μg/m^3 near the construction site.

Wind directions also play a non-negligible effect on the particulate matter (Norra et al., 2023). The influence of wind direction on spatial PM_{10} distribution patterns on 12th July can be seen during the morning bike tour, when wind blew from northeast (Fig. 11). The 24-h backward trajectory also shows the air mass comes from the northeast during the morning tour (Fig. S12). The narrow road towards east–west runs through residential areas in zone 1, the buildings on both sides block the spread of pollutants

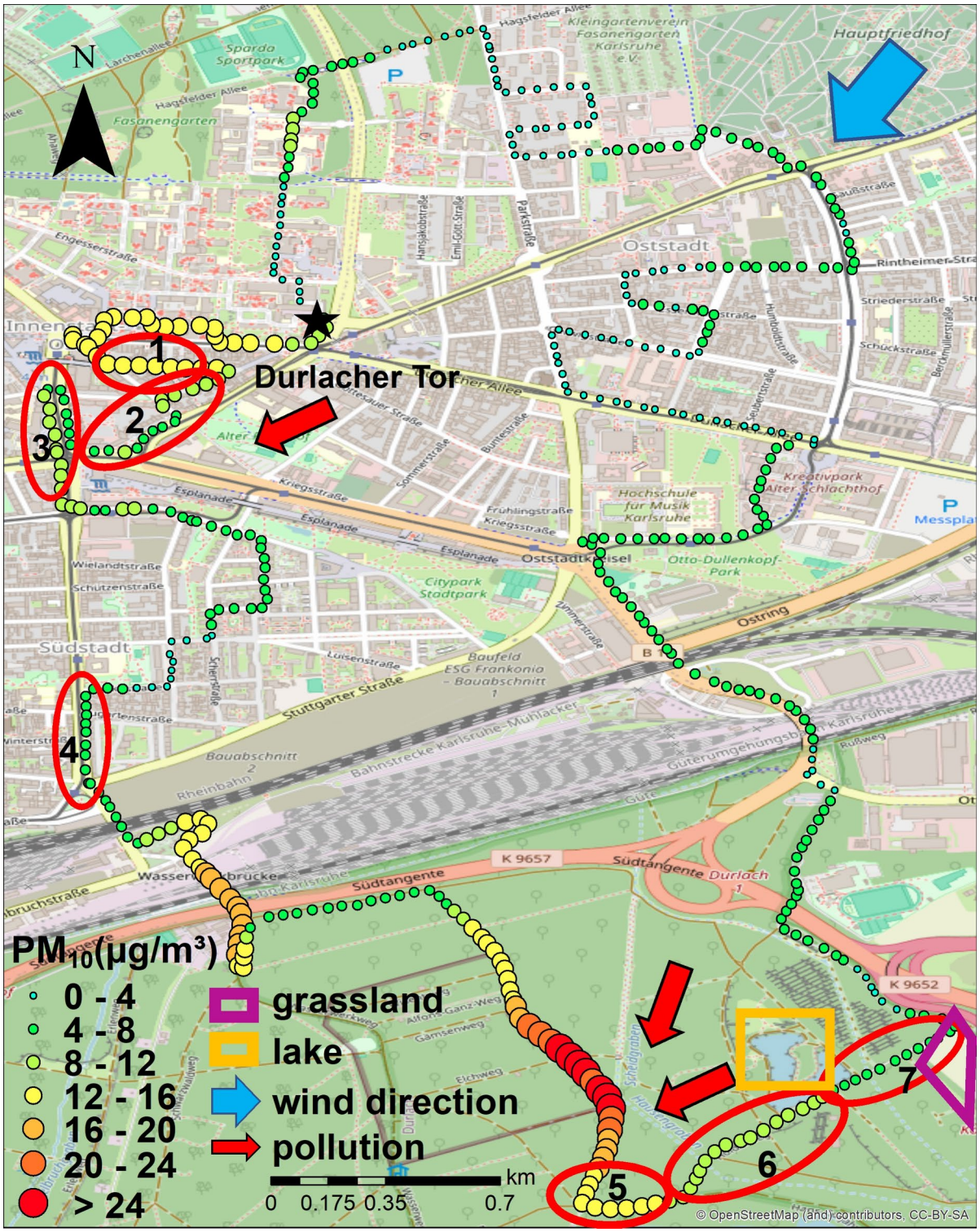

Fig. 11 Interaction of wind direction and particulates matter distribution pattern on 12th of July during the morning tour (see text for numbers)

towards the southwest, and higher concentrations occurs in zone 1. Different particulate matter distribution patterns on two roads towards north-east are parallel to wind direction in zone 2. PM_{10} concentrations on the part of narrow road near to the zone 1 is higher than the part of wide road on the open area (Kriegsstraße) (zone 2, 3). In theory, pollution can be transported along the downwind passage, when encountering obstacles from buildings on both sides and end of the road, aerosols will be blocked to spread and gather (Schmitz et al., 2023). The particulate matter content on the left side of the road is higher than that on the right side in Zone 3. This gives evidence that vehicle emissions and wind-blown aerosols will stop being migrated and accumulated near the downwind end, when the wind is obstructed by buildings. Interestingly, distribution concentrations of aerosols of bike tour show an increasing trend from northeast to southwest in zones 5–7 in the forest. Here, the road located in zones 6–7 formed a narrow wind passage, when road direction is parallel to the wind blew from northeast. It can be seen that lower concentrations occur in the zone 7, that is upwind and close to a flat and open area (lake and grassland area) where aerosols can escape and dilute in a larger air volume. Due to the narrow road pass through the thick forest in the middle part (zone 6), it formed a narrow wind passage. The wind carried aerosols from open area transport along wind passage and as the distance increases. Dense shrub and tree filled the space, which slows down the air flow and leads to increasing in concentrations (Xing & Brimblecombe, 2019). It can be explained that PM concentrations on the road from east to west continue to accumulate. Pollutants from different directions carried by wind that accumulate at intersections in zone 5 higher concentrations occur than in zone 6 and 7. Tong et al. (2015) confirmed that $PM_{2.5}$ concentrations were higher along a transect with trees downwind from the road and declined less sharply than along open transects without trees. Overall, the particulate matter distribution pattern is complex, not only influenced by the wind direction and velocity but also other varying factors, like building structure, human activity, and landscape.

If the higher concentration value of $PM_{2.5}$ (>4.5 μg/m^3) or PM_{10} (>16 μg/m^3) record in a certain segment, we regard this segment as a potential hot spot, and then, this segment appears 3 or more times in 17 sampling campaigns; we consider this segment to be a hot spot. Local hot spots of aerosol concentrations are depicted in Fig. 12 with higher concentration for $PM_{2.5}$ or PM_{10} during the different runs. This means the hot spot areas occurred once or more times the relatively high concentrations level during the 17 bike tours. Traffic light systems play a significant role to keep the efficient operation and safety assurance of cities, but frequent braking on crossroads also increased the emissions of traffic pollutants. Some aerosol hot spots occurred in the crossroads with traffic light system. This picture shows that high-level PM concentrations also occurred in the parking lot areas and rail freight terminal areas. As we mentioned in section of speed effect on potholed path, the underlying surface condition should be regard as a non-negligible factor for rider. We should pay attention to the suspended dust raised by bicycle wheels, especially child cyclist. Lim et al. (2019) found the highest $PM_{2.5}$ concentration levels (55.5 ± 27.7 μg/m^3) located near major roads and highways and the lowest $PM_{2.5}$ concentration level (42.0 ± 24.2 μg/m^3) located the residential areas in Seoul, South Korea. Chauhan et al. (2022) used low-cost sensor which investigated the particulate matter concentration in the northern parts of India. Results indicate that the range of $PM_{2.5}$ concentration is from 20 to 92 μg/m^3 and PM_{10} is from 22 to 131 μg/m^3. Local industries, dust, and crop residue burning are the main sources of pollution. So, the concentrations not only influenced by a single factor but also by the superposition of other factors.

Study limitations

Sampling period in this study was relatively short (17 measurement tours between July 10 and 24, 2022). Therefore, the analysis results could only represent the actual conditions during this specific sampling period. In future work, we will replicate these methods in different seasons to explore broader applicability. The sensor is installed at a low height (60 cm above the ground) and will be affected easily by resuspended dust caused by the wheels when driving on uneven roads. We designed different riding speeds on uneven roads to explore the effect of speed on the resuspended dust caused by the wheels. However, correlation value between speed and $PM_{2.5}$ ($R = 0.21$) and PM_{10} ($R = 0.22$) is weak, and single-day data may

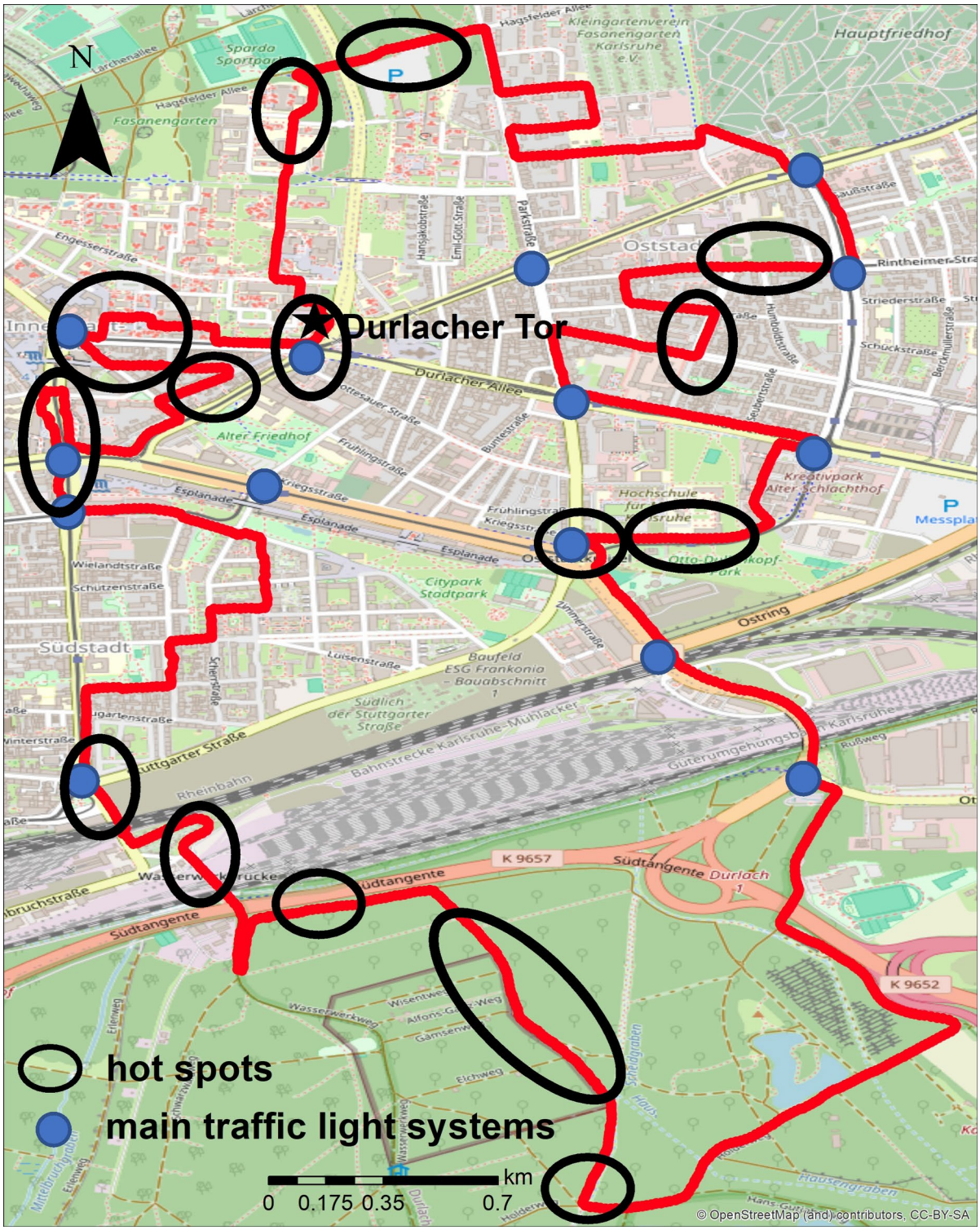

Fig. 12 Hot spots of aerosol pollution recorded by 17 bike tours

limit the strength about speed effects. We did not conduct an in-depth analysis of urban geometric factors, such as building structures and street layouts, which may have more complex implications for the spatial distribution of PM concentrations.

Conclusion

A low-cost particulate sensor OPC_N3 on a bicycle was applied to investigate the PM concentrations in summer time in Karlsruhe. The accuracy of OPC_N3 has been corrected with the Fidas200 and filter samples at the fixed station in Durlacher Tor. The urban environment shows a significant spatio-temporal variation in $PM_{2.5}$ and PM_{10}. In temporal distribution, the mass concentration of $PM_{2.5}$ and PM_{10} measured in the morning was higher than in the afternoon and evening. In spatial distribution, the highest $PM_{2.5}$ and PM_{10} concentrations recorded in the southern forest of Karlsruhe (segment 9), and the underlying surface is the primary influencing factor. Walking at 5 km/h has a higher concentration than speed at 5 km/h of riding. When riding at different speeds on the same gravel and potholes path, higher speed with higher PM concentrations. Major street and street intersection occurred relatively high $PM_{2.5}$ and PM_{10} concentrations. The $PM_{2.5}$ and PM_{10} concentrations in residential area were lower than that in other function areas in Karlsruhe city. $PM_{2.5}$ and PM_{10} concentrations showed different distribution pattern on workday and weekend during the sampling period. Mean $PM_{2.5}$ and PM_{10} concentrations in the morning and evening at weekend are higher than at workday in south forest (segment 10). The PM concentration varies in different residential areas on weekday and weekend during the sampling period. And human activities also have significant effect on the PM mass concentrations, like the construction activity in the Kaiserstraße (segment 1) and a 3-day African Summer Festival in Otto-Dullenkopf Park (segment 13). Besides, the riding speed on gravel and bumpy path has a positive correlation with $PM_{2.5}$ and PM_{10} concentrations.

Consequently, the mobile monitoring with low-cost sensor not only has unmatched flexibility but also can provide the highly spatio-temporal resolution data or even more extra detail for urban aerosol pollution. The low-cost sensor could provide a new perspective for the complex urban study of the air pollution. This case study identifies regularities between aerosol patterns, emission sources, wind speed and building structures.

Acknowledgements Xiao Wang and Junwei Song are thankful for the support from the China Scholarship Council (CSC). We sincerely appreciate the anonymous reviewers for their patience in reviewing the paper and their constructive comments and suggestions.

Author contribution Xiao Wang: data collection, methodology, manuscript preparation; Junwei Song: methodology development, manuscript reviewing; Harald Saathoff: experimental equipment providing, manuscript reviewing; Reiner Gebhardt: experimental equipment providing, methodology development; Stefan Norra: supervision, methodology, manuscript reviewing.

Funding This research has been supported by the China Scholarship Council (CSC) with project number CSC202106400009.

Data availability No datasets were generated or analysed during the current study.

Declarations

Competing interests The authors declare no competing interests.

References

Aix, M.-L., Schmitz, S., & Bicout, D. J. (2023). Calibration methodology of low-cost sensors for high-quality monitoring of fine particulate matter. *Science of the Total Environment, 889*, 164063. https://doi.org/10.1016/j.scitotenv.2023.164063

Birmili, W., Rehn, J., Vogel, A., Boehlke, C., Weber, K., & Rasch, F. (2013). Micro-scale variability of urban particle number and mass concentrations in Leipzig, Germany. *Meteorologische Zeitschrift, 22*, 155–165. https://doi.org/10.1127/0941-2948/2013/0394

Carreras, H., Ehrnsperger, L., Klemm, O., & Paas, B. (2020). Cyclists' exposure to air pollution: In situ evaluation with a cargo bike platform. *Environmental Monitoring and Assessment192*, 470https://doi.org/10.1007/s10661-020-08443-7

Chauhan, A., Singh, R. P., Matsumi, Y., Hayashida, S., Nakayama, T., Gupta, S. K., & Shukla, D. P. (2022). Variability of the particulate matter concentration in the northern parts of India using low-cost sensors. *In: Int Geosci Remote Sens Symp 2022-July*, 6686–6689. https://doi.org/10.1109/IGARSS46834.2022.9884246

Choi, W., Hu, S., He, M., Kozawa, K., Mara, S., Winer, A. M., & Paulson, S. E. (2013). Neighborhood-scale air quality

impacts of emissions from motor vehicles and aircraft. *Atmospheric Environment, 80*, 310–321. https://doi.org/10.1016/j.atmosenv.2013.07.043

Chu, B., Zhang, S. P., Liu, J., Ma, Q. X., & He, H. (2021). Significant concurrent decrease in PM2.5 and NO2 concentrations in China during COVID-19 epidemic. *Journal of Environmental Sciences, 99*, 346–353. https://doi.org/10.1016/j.jes.2020.06.031

Cummings, L. E., Stewart, J. D., Reist, R., Shakya, K. M., & Kremer, P. (2021). Mobile monitoring of air pollution reveals spatial and temporal variation in an urban landscape. *Frontiers in Built Environment, 7*, 648620. https://doi.org/10.3389/fbuil.2021.648620

Dacre, H. F., Mortimer, A. H., & Neal, L. S. (2020). How have surface NO_2 concentrations changed as a result of the UK's COVID-19 travel restrictions? *Environmental Research Letters, 15*, 104089. https://doi.org/10.1088/1748-9326/abb6a2

Dubey, R., Patra, A. K., Joshi, J., Blankenberg, D., Kolluru, S. S. R., Madhu, B., & Raval, S. (2022). Evaluation of low-cost particulate matter sensors OPC N2 and PM Nova for aerosol monitoring. *Atmospheric Pollution Research, 13*(3), 101335. https://doi.org/10.1016/j.apr.2022.101335

Ghahremanloo, M., Lops, Y., Choi, Y., Jung, J., Mousavinezhad, S., & Hammond, D., (2022). A comprehensive study of the COVID-19 impact on $PM_{2.5}$ levels over the contiguous United States: A deep learning approach. *Atmospheric Environment,* 272, 118944. https://doi.org/10.1016/j.atmosenv.2022.118944

Kang, J., & Choi, K. (2024). Calibration methods for low-cost particulate matter sensors considering seasonal variability. *Sensors, 24*(10), 3023. https://doi.org/10.3390/s24103023

Karagulian, F., Barbiere, M., Kotsev, A., Spinelle, L., Gerboles, M., Lagler, F., Redon, N., Crunaire, S., & Borowiak, A. (2019). Review of the performance of low-cost sensors for air quality monitoring. *Atmosphere, 10*(9), 506. https://doi.org/10.3390/atmos10090506

Levy, Z. M., Xiong, F., Gentner, D., Kerkez, B., Kohrman-Glaser, J., & Koehler, K. (2019). Field and laboratory evaluations of the low-cost plantower particulate matter sensor. *Environmental Science & Technology, 53*, 838–849. https://doi.org/10.1021/acs.est.8b05174

Lim, C. C., Kim, H., Vilcassim, M. J. R., Thurston, G. D., Gordon, T., Chen, L., Lee, K., Heimbinder, M., & Kim, S. Y. (2019). Mapping urban air quality using mobile sampling with low-cost sensors and machine learning in Seoul. *South Korea. Environment International, 131*, 105022. https://doi.org/10.1016/j.envint.2019.105022

Liu, X., Zhang, X., Schnelle-Kreis, J., Jakobi, G., Cao, X., Cyrys, J., Yang, L., Schloter-Hai, B., Abbaszade, G., Orasche, J., Khedr, M., Kowalski, M., Hank, M., & Zimmermann, R. (2021). Spatiotemporal characteristics and driving factors of black carbon in Augsburg, Germany: Combination of mobile monitoring and street view images. *Environmental Science & Technology, 55*(1), 160–168. https://doi.org/10.1021/acs.est.0c04776

Mueller, W., Wilkinson, P., Milner, J., Loh, M., Vardoulakis, S., Petard, Z., Cherrie, M., Puttaswamy, N., Balakrishnan, K., & Arvind, D.K. (2022) The relationship between greenspace and personal exposure to $PM_{2.5}$ during walking trips in Delhi, India. *Environmental Pollution,* 305, 119294. https://doi.org/10.1016/j.envpol.2022.119294

Norra, S., Song, J., Gebhardt, R., Bauer, J., Broß, M., Fuchs, M., Huber, T., Macj, D., & Saathoff, H. (2023). Spatiotemporal dynamics of aerosol distribution in an urban environment recorded in situ by means of a bike based monitoring system. *Frontiers in Environmental Science, 11*, 749477. https://doi.org/10.3389/fenvs.2023.749477

Páez-Osuna, F., Valencia-Castañeda, G., & Rebolledo, U. A. (2022). The link between COVID-19 mortality and $PM_{2.5}$ emissions in rural and medium-size municipalities considering population density, dust events, and wind speed. *Chemosphere,* 286, 131634. https://doi.org/10.1016/j.chemosphere.2021.131634

Pattinson, W., Longley, I., & Kingham, S. (2014). Using mobile monitoring to visualise diurnal variation of traffic pollutants across two near-highway neighbourhoods. *Atmospheric Environment, 94*, 782–792. https://doi.org/10.1016/j.atmosenv.2014.06.007

Peters, J., Van den Bossche, J., Reggente, M., Van Poppel, M., De Baets, B., & Theunis, J. (2014). Cyclist exposure to UFP and BC on urban routes in Antwerp, Belgium. *Atmospheric Environment, 92*, 31–43. https://doi.org/10.1016/j.atmosenv.2014.03.039

Pochwała, S., Gardecki, A., Lewandowski, P., Somogyi, V., & Anweiler, S. (2020). Developing of low-cost air pollution sensor—measurements with the unmanned aerial vehicles in Poland. *Sensors, 20*(12), 3582. https://doi.org/10.3390/s20123582

Rodes, C. E., Kamens, R. M., & Wiener, R. W. (1991). The significance and characteristics of the personal activity cloud on exposure assessment measurements for indoor contaminants. *Indoor Air, 1*(2), 123–145. https://doi.org/10.1111/j.1600-0668.1991.03-12.x

Samad, A., & Vogt, U. (2020). Investigation of urban air quality by performing mobile measurements using a bicycle (MOBAIR). *Urban Climate, 33*, 100650. https://doi.org/10.1016/j.uclim.2020.100650

Schmitz, S., Villena, G., Caseiro, A., Meier, F., Kerschbaumer, A., & Schneidemesser, E. (2023). Calibrating low-cost sensors to measure vertical and horizontal gradients of NO_2 and O_3 pollution in three street canyons in Berlin. *Atmospheric Environment, 307*, 119830. https://doi.org/10.1016/j.atmosenv.2023.119830

Shi, Z., Song, C., Liu, B., Lu, G., Xu, J., Vu, T.V., Elliott, R. J. R., Li, W., Bloss, W. J., & Harrison, R. M. (2021). Abrupt but smaller than expected changes in surface air quality attributable to COVID-19 lockdowns. *Science Advances,* 7(3), eabd6696. https://doi.org/10.1126/sciadv.abd6696

Song, J., Saathoff, H., Gao, L., Gebhardt, R., Jiang, F., Vallon, M., Bauer, J., Norra, S., & Leisner, S. (2022). Variations of $PM_{2.5}$ sources in the context of meteorology and seasonality at an urban street canyon in Southwest Germany. *Atmospheric Environment,* 282, 119147. https://doi.org/10.1016/j.atmosenv.2022.119147

Stadt Karlsruhe (2013). Verkehrsentwicklungsplan Karlsruhe zustandsanalyse. Karlsruhe: Stadtplanungsamt Karlsruhe.

Tong, Z., Whitlow, T. H., MacRae, P. F., Landers, A. J., & Harada, Y. (2015). Quantifying the effect of vegetation on near-road air quality using brief campaigns.

Environmental Pollution, 201, 141–149. https://doi.org/10.1016/j.envpol.2015.02.026

Wu, D., Zhang, G. C., Liu, J. Q., Shen, S. Y. Yang, Z. Q., Pan, Y. T., Zhao, X. N., Yang, S. Y., Tian, Y., Zhao, H. D., Li, J. J., & Cai, L.(2022). Influence of particle properties and environmental factors on the performance of typical particle monitors and low-cost particle sensors in the market of China. *Atmospheric Environment,* 268, 118825. https://doi.org/10.1016/j.atmosenv.2021.118825

Xing, Y., & Brimblecombe, P. (2019). Role of vegetation in deposition and dispersion of air pollution in urban parks. *Atmospheric Environment, 201*, 73–83. https://doi.org/10.1016/j.atmosenv.2018.12.027

Zeindl, L., & Koenigstorfer, J. (2020). Health benefit assessment of running in urban areas against the background of particulate matter 2.5 concentration: the Munich Olympic Park. *Urban Science,* 4(4), 62. https://doi.org/10.3390/urbansci4040062

Zikova, N., Hopke, P. K., & Ferro, A. R. (2017). Evaluation of new low-cost particle monitors for $PM_{2.5}$ concentrations measurements. *Journal of Aerosol Science, 105*, 24–34. https://doi.org/10.1016/j.jaerosci.2016.11.010